Reassociation of the Pyruvate Dehydrogenase Complex from *Escherichia coli*: Kinetic Measurements and Binding Studies by Resonance Energy Transfer†

Klaus Graupe, Mahmut Abusaud, Heinrich Karfunkel,‡ and Hans Bisswanger*

ABSTRACT: The reassociation of the pyruvate dehydrogenase complex of *Escherichia coli* from pyruvate dehydrogenase (E1) and the dihydrolipoamide transacetylase–dihydrolipoamide dehydrogenase subcomplex (E2E3) has been studied by observing the reappearance of overall enzymatic activity of the complex and by resonance energy transfer. The restoration of the overall activity occurs after a pronounced lag in the range of seconds. The lag reflects the approach to equilibrium in the assembly of the complex. A simple second-order binding of the two enzyme components can be excluded; the mechanism consists rather of a rapid binding step followed by a slow isomerization. The E1 component binds to the subcomplex in an anticooperative manner. The association constant for the binding of the first subunit is $K_{a1} = 3.6 \times 10^8$ M^{-1} and that for the final subunit binding is $K_{af} = 8 \times 10^7$ M^{-1}. When the components are allowed to preincubate for a longer time, the anticooperative binding function changes to a hyperbolic one with a highly increased affinity constant of $K_a = 9.5 \times 10^{10}$ M^{-1}. Independent of the mode of binding, the binding of one E1 dimer to one E2E2 protomer is consonant with a limiting polypeptide chain stoichiometry of 2:1:1 for the three enzyme components E1:E2:E3. The anticooperative binding behavior of the E1 component was confirmed by measurement of the nearest neighborhood of chromophore-labeled E1 subunits on the surface of the E2E3 subcomplex with the aid of resonance energy transfer. Theoretical binding functions were calculated by a Monte-Carlo computer simulation in order to interpret the saturation function obtained by this technique. The results suggest that the initial binding of E1 subunits to the E2E3 subcomplex can lead to the production of a metastable complex in which the unfavorable E1–E1 interactions (most probably steric hindrance) are present. This metastable complex slowly rearranges to yield a more stable complex.

The pyruvate dehydrogenase complex catalyzes the oxidative decarboxylation of pyruvate in a multistep reaction (Koike et al., 1963). Three enzyme components participate in the overall reaction:

$$\text{pyruvate} + \text{NAD}^+ + \text{CoA–SH} \rightarrow \text{acetyl–CoA} + \text{CO}_2 + \text{NADH} + \text{H}^+$$

i.e., pyruvate dehydrogenase (E1),[1] dihydrolipoamide transacetylase (E2), and dihydrolipoamide dehydrogenase (E3).

In *Escherichia coli* multiple copies of each component are integrated into a multienzyme complex (Reed, 1974). The exact number of the polypeptide chains is still controversial; chain stoichiometries of E1:E2:E3 = 48:24:24, 24:24:12, or 16:16:16 are discussed (Vogel et al., 1972a,b; Bates et al., 1975, 1977; Reed et al., 1975; Perham & Hooper, 1977; Angelides et al., 1979; Danson et al., 1979). The complex may be separated into its three enzyme components. The molecular weights of the individual polypeptide chains are 100000 (E1), 83000 (E2), and 56000 (E3) (Perham & Thomas, 1971; Vogel et al., 1972b; Vogel, 1977). Both isolated E1 and E3 components exist as stable dimers (Vogel & Henning, 1971; Eley et al., 1972).

The self-assembly of the pyruvate dehydrogenase complex from *Escherichia coli* has previously been investigated in order to determine the polypeptide chain stoichiometry (Reed et al., 1975; Bates et al., 1977). In this paper we report kinetic and equilibrium studies of the reassembly of the pyruvate dehydrogenase complex from the E1 component and an E2E3 subcomplex. This study employed fluorescence energy transfer as a technique for preferentially observing the interaction of E1 subunits adjacent to one another in the reconstituted pyruvate dehydrogenase complex.

Materials and Methods

Chemicals. All chemicals used were of the highest available purity. Enzymes, cofactors, and enzyme substrates were from Boehringer Mannheim, GFR. Celite 535 was bought from Serva, Heidelberg, and Sephadex G-25 and G-50 were from Pharmacia, Uppsala, Sweden. Cellulose CF-11 was obtained from Whatman, Maidstone, KY, and fluorescein isothiocyanate was from Fluka, Buchs, Switzerland. 2-Methoxy-2,4-diphenyl-3(2*H*)-furanone (MDPF) was kindly donated by Hoffmann-La Roche, Basel, Switzerland.

The pyruvate dehydrogenase component (E1) was isolated from the mutant *aceF*10 of *E. coli* K12 according to Saumweber et al. (1981). The pyruvate dehydrogenase complex was purified from the wild-type strain *Ymel* of *E. coli* K12 as described by Bisswanger (1981). This method was also applied to purify the E2E3 subcomplex from the mutant *aceE*2, which is defective in the structural gene of the pyruvate dehydrogenase component (Henning & Herz, 1964).

Alternatively the E2E3 subcomplex was obtained from purified pyruvate dehydrogenase complex by a rapid ultracentrifugation procedure. Purified pyruvate dehydrogenase complex in 0.1 M potassium phosphate buffer, pH 7.6 (10 mg/mL), was sedimented by centrifugation for 20 min at 135000*g* in an air-driven ultracentrifuge (Airfuge, Beckman,

† From the Physiologisch-chemisches Institut der Universität Tübingen, D-7400 Tübingen, West Germany. *Received May 27, 1981.* This work was supported by a grant of the Deutsche Forschungsgemeinschaft.

‡ Present address: Institut für Theoretische Chemie der Universität Tübingen, D-7400 Tübingen, West Germany.

[1] Abbreviations: E1, pyruvate dehydrogenase; E2, dihydrolipoamide transacetylase; E3, dihydrolipoamide dehydrogenase; TPP, thiamine diphosphate; CoA, coenzyme A; FITC, fluorescein isothiocyanate; MDPF, 2-methoxy-2,4-diphenyl-3(2*H*)-furanone; NADH, reduced nicotinamide adenine dinucleotide; NAD, nicotinamide adenine dinucleotide; PC, active E1E2E3 protomer; PC′, inactive E1E2E3 protomer; $\bar{Y}$, fractional saturation; n, number of binding sites; K_a^+, association constant for complex formation; K_{a1}, association constant for binding of the first subunit; K_{af}, association constant for binding of the final subunit; K_{ai}, equilibrium constant of the isomerization process; k_c, catalytic constant.

0006-2960/82/0421-1386$01.25/0

Palo Alto, CA). The supernatant was carefully removed. The pellet was dissolved in 20 mM sodium carbonate buffer, pH 10, and centrifuged again for 20 min at 135000*g*. The supernatant containing the E1 component was collected. The pellet was redissolved in the sodium carbonate buffer and centrifuged once more. This procedure was repeated 3 times. Finally the pellet was dissolved in 0.1 M potassium phosphate buffer, pH 7.6. An overall enzymatic activity of 0.2–0.5% compared to the native enzyme complex remains with the isolated E2E3 subcomplex.

Enzyme Tests and Protein Determination. For steady-state measurements of the overall enzymatic reaction the formation of NADH was followed with a Varian Techtron 635 spectrophotometer (Varian Techtron, Melbourne, Australia) according to Schwartz et al. (1968). Activity was quantified in micromoles of NADH produced per minute at 37 °C. The specific activity of the purified pyruvate dehydrogenase complex was 38 units/mg; that of the restored enzyme complexes ranged between 34.5 and 38 units/mg. Protein determination was performed according to the method of Lowry et al. (1951) as modified by Hartree (1972).

Fluorescence Labeling. Fluorescein isothiocyanate was coupled to the E1 component according to Scouten et al. (1974). Briefly, 20 mg of the dye was dissolved in 5 mL of acetone. Cellulose CF-11 (1 g) was added and the solution was stirred until all the acetone had evaporated. Finally the cellulose was dried under vacuum. The enzyme solution (1 mg in 2 mL of 0.1 M potassium phosphate buffer, pH 7.6) was mixed with 10 mg of the cellulose to which the dye had adsorbed. The mixture was gently shaken for 8 h at 4 °C. Then the cellulose was removed by centrifugation. Excess reagent was removed by gel filtration on a 1 × 14 cm Sephadex G-25 column using 0.1 M potassium phosphate buffer for equilibration and elution.

The pyruvate dehydrogenase component was labeled with MDPF by a slight modification of the Rinderknecht method (Rinderknecht, 1962). The MDPF–celite was prepared according to Weigele et al. (1973). MDPF–celite (2 mg, containing 20% dye) was mixed rapidly with enzyme solution (1 mg in 2 mL of 0.1 M potassium phosphate buffer, adjusted to pH 8.9 with 20 mM sodium carbonate buffer, pH 10) and shaken for 12 min at room temperature. The mixture was centrifuged and the supernatant applied to a 1 × 42 cm Sephadex G-50 column equilibrated with 0.1 M potassium phosphate buffer, pH 7.6. The labeled enzyme was separated from unreacted dye by elution with the same buffer.

Average degree of labeling, i.e., moles of dye bound per mole of enzyme, was determined by measuring the absorption of the bound dye and the protein concentration. Molar absorption coefficients used for the bound dyes were $\epsilon^{385}_{MDPF} = 6400\ M^{-1}\ cm^{-1}$ (Handschin & Ritschard, 1976) and $\epsilon^{495}_{FITC} = 4.25 \times 10^4\ M^{-1}\ cm^{-1}$ (Tengerdy & Chang, 1966).

Fluorescence energy transfer measurements were performed on a Farrand MK1 spectrofluorometer (Farrand Inc., Valhalla, NY) connected to a Philips PM 8131 XY recorder (Philips, Kasssel, GFR).

Monte-Carlo Simulation. The binding of the E1 component to the E2E3 subcomplex was calculated by computer simulation by the aid of the Monte-Carlo method (Hammersley & Handscomb, 1965). For simplicity the E2E3 subcomplex was assumed to be a flat disk possessing 20 equivalent binding sites along the periphery. The value of 20 was chosen as the mean between the 16 E1 components found by Vogel et al. (1972b) and the value of 24 E1 polypeptide chains proposed by Reed et al. (1975), Angelides et al. (1979), and Danson et al. (1979). For binding of the E1 subunits two different situations were distinguished: (i) binding to a site whose neighboring sites were still unoccupied (unhindered sites); (ii) binding to a site adjacent to one or two previously bound E1 subunits (hindered sites, no further differentiation is made between sites with one or two direct neighbors). The relative probability of occupying unhindered sites as well as the probability of independent (normal) binding to hindered sites was assumed to be $P = 1$. Cooperative binding to hindered sites has a probability of $P > 1$, for anticooperative binding is $P < 1$. The ligands were divided into two classes, corresponding to the two different labeled pyruvate dehydrogenase components. They were to be indistinguishable in their binding properties.

Initially the disks were occupied via Monte-Carlo simulation only to a certain extent by one class of ligands, that is, $^1/_{20}$ of the total of binding sites, corresponding to about 1 ligand molecule/disk. Then ligands of the other class were added stepwise until complete saturation of the disks. After each binding step the number of possible pairs formed by the two different types of ligands was counted and recorded as a function of the number of binding sites already occupied. Each ligand was counted only once. Since the calculation is not totally unambiguous (the mistake being very small though), the count was started from two different positions on the disk, and the higher number of pairs was always chosen. The simulation was carried out with 100 disk molecules and repeated 10 times, and finally the mean values were computed.

Theory

The formation of the native pyruvate dehydrogenase complex from the E1 component and the E2E3 subcomplex was monitored by observing the restoration of the catalytic activity, i.e., the NAD-dependent reduction of pyruvate. The progress curves of this process show a noticeable lag followed by a strictly linear steady-state region. The time constant of this lag τ_0 is defined as the intercept of the steady-state line extrapolated back to the time axis. τ_0 should be a complex function of the different rate constants involved in the mechanism of the overall reassembly process (Gutfreund, 1972; Strickland et al., 1975).

The most simple mechanism of reassembly is described by (mechanism I)

$$E1 + E2E3 \underset{k_{-1}}{\overset{k_1}{\rightleftharpoons}} PC \qquad (I)$$

where E1 is the pyruvate dehydrogenase subunit, E2E3 is a protomer of the E2E3 subcomplex with one binding site for the E1 subunit, and PC is an active E1E2E3 protomer. Provided that pseudo-first-order conditions $[E1]_0 \ll [E2E3] \sim [E2E3]_0$ are obtained, the concentration of PC at time t is given by

$$[PC]_t = (a/b)(1 - e^{-bt}) \qquad (1)$$

with $a = k_1[E2E3]_0[E1]_0$ and $b = k_1[E2E3]_0 + k_{-1}$ (the subscript "0" designates initial concentrations at $t = 0$).

Presuming that each E1 subunit bound to the complex molecule contributes equally to the overall activity, at saturating amounts of all substrates and cofactors necessary for the catalytic reaction the rate of NADH formation is

$$\frac{d[NADH]}{dt} = V = k_c[PC]_t \qquad (2)$$

where k_c is the catalytic rate constant. By integration one obtains from eq 1 and 2 the concentration of the product NADH at time t:

$$[NADH]_t = (k_c ta/b) - [k_c(1 - e^{-bt})a/b^2] \quad (3)$$

For the steady-state phase (ss, $t \rightarrow \infty$) the exponential term can be neglected; thus

$$[NADH]_{ss,t} = (k_c ta/b) - (k_c a/b^2) \quad (4)$$

and, since for $[NADH]_{ss,t} = 0$ t becomes τ_0, the time constant of the lag period is

$$\tau_0 = \frac{1}{k_1[E2E3]_0 + k_{-1}} \quad (5)$$

From eq 5 it follows that a strict linear relationship between $1/\tau_0$ and $[E2E3]_0$ is expected.

A bimolecular reassembly mechanism followed by an isomerization step of the enzyme complex, where PC′ is an inactive and PC the active enzyme conformation (mechanism II)

$$E1 + E2E3 \underset{k_{-1}}{\overset{k_1}{\rightleftharpoons}} PC' \underset{k_{-2}}{\overset{k_2}{\rightleftharpoons}} PC \quad (II)$$

may be treated in an analogous manner (Strickland et al., 1975). Assuming the initial binding step to be rapid compared to the isomerization reaction, i.e., $k_2 \ll k_{-1}$, the concentration of PC at time t is

$$[PC]_t = (c/d)(1 - e^{-dt/f}) \quad (6)$$

The concentration of the product at time t is

$$[NADH]_t = (k_c tc/d) - [k_c(1 - e^{-dt/f})cf/d^2] \quad (7)$$

for $c = k_1k_2[E1]_0[E2E3]_0$, $d = k_1k_2[E2E3]_0 + k_{-2}(k_1[E2E3]_0 + k_{-1})$, and $f = k_1[E2E3]_0 + k_{-1}$. $1/\tau_0$ becomes

$$\frac{1}{\tau_0} = \frac{d}{f} = \frac{k_1k_2[E2E3]_0}{k_1[E2E3]_0 + k_{-1}} + k_{-2} \quad (8)$$

In this case a linear dependence of $1/\tau_0$ on $[E2E3]_0$ is expected only when $k_1[E2E3]_0 \ll k_{-1}$. Equation 8 may be linearized by rearrangement to

$$\frac{1}{1/\tau_0 - k_{-2}} = \frac{1}{k_2} + \frac{k_{-1}}{k_1k_2}\frac{1}{[E2E3]_0} \quad (9)$$

Results

Kinetics of the Reassembly Process. Reassociation of the isolated E1 component with the E2E3 subcomplex reconstitutes the enzyme complex, which resembles in structure and enzyme activity the native pyruvate dehydrogenase complex (Koike et al., 1963; Fernandez-Moran et al., 1964). Thus the appearance of enzymatic activity is an indication of the restoration of the native structure, and the rate of substrate utilization is proportional to the amount of active complex formed.

The E1 component and the E2E3 subcomplex were mixed in the presence of the substrate and cofactors necessary for the overall catalytic reaction of the pyruvate dehydrogenase complex, and the rate of NADH production was monitored. In repeated experiments specific activities of 90–100% compared to the unresolved pyruvate dehydrogenase complex were observed for the reconstituted enzymes. The progress curves exhibit an initial lag period of several seconds before the rate of NAD reduction attains a constant value. Since, under the same experimental conditions, no such lag period can be observed when the reaction was started with the native enzyme complex, this lag is attributable to the reassembly of the complex. Two simple models are considered: a bimolecular reaction, whereby the active conformation may be obtained in one single step (mechanism I; cf. Theory), or an association to yield an inactive intermediate, followed by an isomerization to the active complex (mechanism II). The subcomplex is assumed to consist of E2E3 protomers, the protomer being defined as a heterologous dimer of one E2 and one E3 polypeptide chain with a molecular weight of together 139 000. As described above, the number of protomers present in the complex is not yet clear.

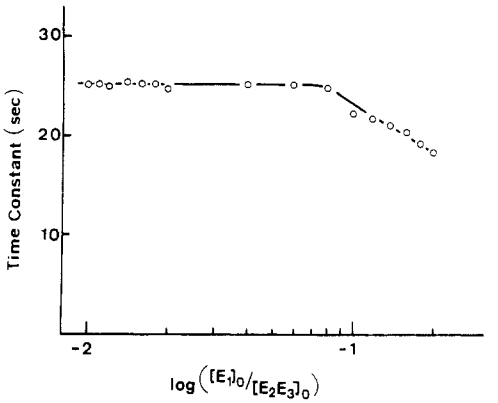

FIGURE 1: Dependence of the time constant τ_0 of the lag period on the concentration of the pyruvate dehydrogenase component (E1). Increasing amounts of the E1 component were incubated for 2 min at 37 °C in 1 mL of test mixture (NAD omitted) for the overall catalytic reaction of the pyruvate dehydrogenase complex. The reaction was started by simultaneous addition of 2.5 mM NAD and 4.1×10^{-8} M protomers of E2E3 subcomplex. τ_0 is obtained from the progress curves of the catalytic reaction as is described under Theory.

As is shown under Theory, the time constant τ_0 of the lag period should be independent of the concentration of E1 for both mechanisms discussed above, as long as true pseudo-first-order conditions ($[E1] \ll [E2E3]$) prevail. To test this assertion, we studied the reassociation process with a constant amount of E2E3 subcomplex and varying concentrations of the E1 component. The E1 component was incubated for about 2 min with the test mixture for the overall reaction, omitting NAD. This preincubation time of the E1 component, however, is not essential, and no significant change of the lag period was observed when the incubation time varies by a few minutes. NAD was added together with the E2E3 subcomplex to start the reaction. The time constant of the lag was determined as is described under Theory from the progress curves of the overall enzyme reaction. Figure 1 shows clearly that at low ratios of E1 component to subcomplex protomer a constant value of τ_0 was obtained, while a decrease of τ_0 appears at higher ratios, where pseudo-first-order conditions no longer exist.

To differentiate between a simple second-order reassociation process (mechanism I) and a reassociation followed by a rate-determining isomerization (mechanism II), we repeated the experiment described above leaving the E1 component constant and varying the amount of the E2E3 subcomplex. These data are plotted in Figure 2. At low concentrations of subcomplex a linear dependence of $1/\tau_0$ on the concentration of the E2E3 protomer is observed, whereas at higher concentrations a clear deviation from linearity is found (Figure 2A). This behavior excludes a simple second-order mechanism, which should show strict linearity (cf. eq 5), but is in accordance with the rapid binding–slow isomerization process (eq 8). From the intercept of the curve on the ordinate a first-order rate constant of $k_{-2} = 7.9 \times 10^{-3}$ s^{-1} can be calculated according to eq 8. As is expected from eq 9 the data can be linearized in a plot as depicted in Figure 2B. The values of $k_2 = 1.9$ s^{-1} from the intercept and of the association constant of $K_a^+ = k_1/k_{-1} = 1.5 \times 10^6$ M^{-1} from the slope of the line are determined.

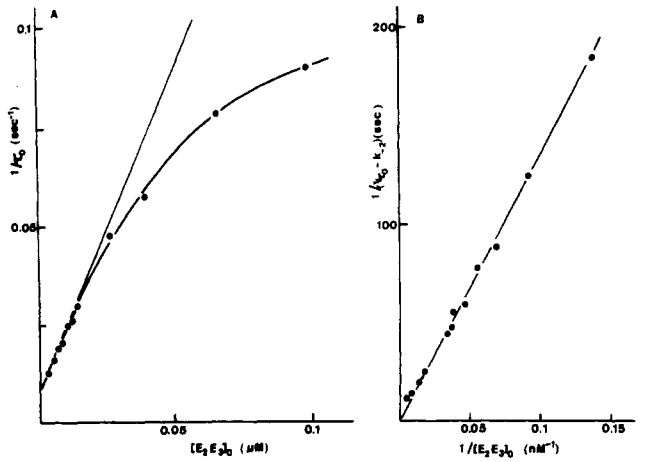

FIGURE 2: Reassociation of the E1 component with E2E3 subcomplex under pseudo-first-order conditions. The E1 component (0.6 nM) was added to 1 mL of test mixture (NAD omitted). The reaction was started by adding 2.5 mM NAD and E2E3 subcomplex as indicated on the abscissa. The reciprocal value of τ_0 is plotted against the concentration of the E2E3 protomer in (A). The curve is linearized according to eq 9 in (B).

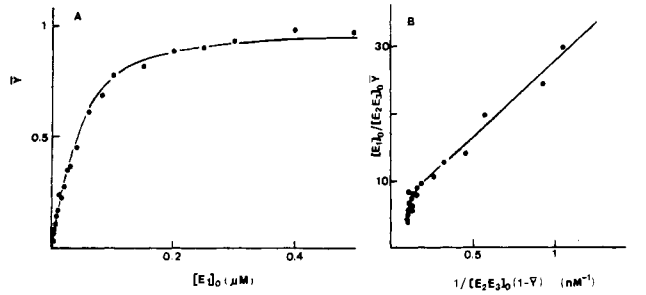

FIGURE 3: Binding of the pyruvate dehydrogenase component (E1) to the E2E3 subcomplex as determined by steady-state measurements. E1 in different concentrations as indicated on the abscissa was incubated with test mixture (NAD omitted) for 2 min and the enzyme reaction started with 2.5 mM NAD and 1.1×10^{-8} M E2E3 protomers. The steady-state rate obtained from the progress curves is plotted as fractional saturation $\bar{Y} = v/V$ vs. the E1 monomer concentration in (A) and replotted according to Stockell (1959) in (B).

The dependence of $1/\tau_0$ upon the concentration of the subcomplex indicated that the lag period in fact reflects the approach to equilibrium in the reassembly process. This justifies regarding the steady-state reaction rate as a direct measure of the degree of restoration of active enzyme structure.

Binding Studies by Steady-State Measurements without Preincubation. To follow the binding process of E1 to the E2E3 subcomplex, we added increasing amounts of the isolated component to a constant amount of the subcomplex, together with the test mixture of the overall reaction. The slope of the linear steady-state region of the progress curves is plotted against the E1 concentration as is depicted in Figure 3A. An apparently normal titration curve is seen. This curve can be linearized in the manner of Stockell (1959) on the basis of the binding equation of Klotz (1946):

$$\frac{[E1]_0}{[E2E3]_0}\frac{1}{\bar{Y}} = n + \frac{1}{K_a}\frac{1}{[E2E3]_0(1-\bar{Y})} \qquad (10)$$

$\bar{Y} = v/V$ and is the fractional saturation, K_a is the intrinsic association constant, and n is the number of binding sites. However, as can be seen from Figure 3B, a clear deviation from linearity is noticeable. A curved function is obtained up to about 70% saturation of the subcomplex with the E1 component. This region is followed by a linear part in the higher saturation range. To understand deviations of this type, we derived a general expression of the slope of the curves in the diagram of Stockell, employing the Adair equation (Adair, 1925). This is shown in detail in the Appendix. The analysis suggests that the curvature observed in our experiment is characteristic of anticooperative binding behavior. From the linear portion of the binding curve an association constant for the final binding step of one E1 subunit to the E2E3 protomer of $K_{af} = 8 \times 10^7$ M^{-1} can be calculated.

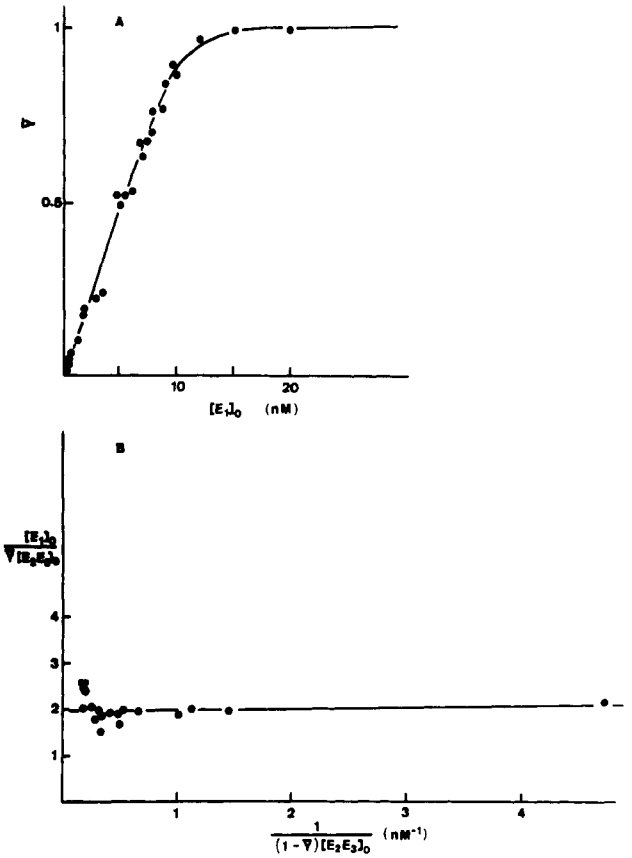

FIGURE 4: Determination of binding of E1 subunits to E2E3 subcomplex after preincubation of the components. E2E3 subcomplex (6.33×10^{-9} M) was preincubated with various amounts of E1 component as indicated on the abscissa in 1 mL of 0.1 M potassium phosphate buffer, pH 7.6, at 0 °C for 18 h. Thereafter 20 μL of a concentrated test mixture (pyruvate omitted) was added to give the final cofactor concentrations for the enzyme test in the cuvette. The reaction was started by addition of pyruvate. The steady-state reaction rate is plotted directly against the concentration of the E1 chains in (A); Stockell diagram is shown in (B).

Binding Studies by Steady-State Measurements with Preincubation. In a second set of experiments the E2E3 subcomplex was preincubated with varying amounts of the E1 component for 18 h at 4 °C. The start of the overall reaction of the pyruvate dehydrogenase complex proceeds without detectable lag period, and a linear initial steady-state rate was observed in all cases. Plotting the E1 concentrations against the steady-state rate yields a normal titration curve (Figure 4A), and in the Stockell diagram a straight line is obtained throughout (Figure 4B). A scattering of the data around this line at very low E1 concentrations is due to the slow rates under these conditions and to the special plotting mode. From the intercept of the line in this diagram one binding site for one E1 dimer on each E2E3 protomer is calculated, and from the slope an association constant of $K_a = 9.5 \times 10^{10}$ M^{-1} is obtained.

Binding Studies by Fluorescence Energy Transfer Measurements. Fluorescence energy transfer has been employed to determine distances of reactive centers on macromolecules, maximum distance for efficient energy transfer usually being in the range of 6 nm (Förster, 1948; Stryer & Haugland, 1967;

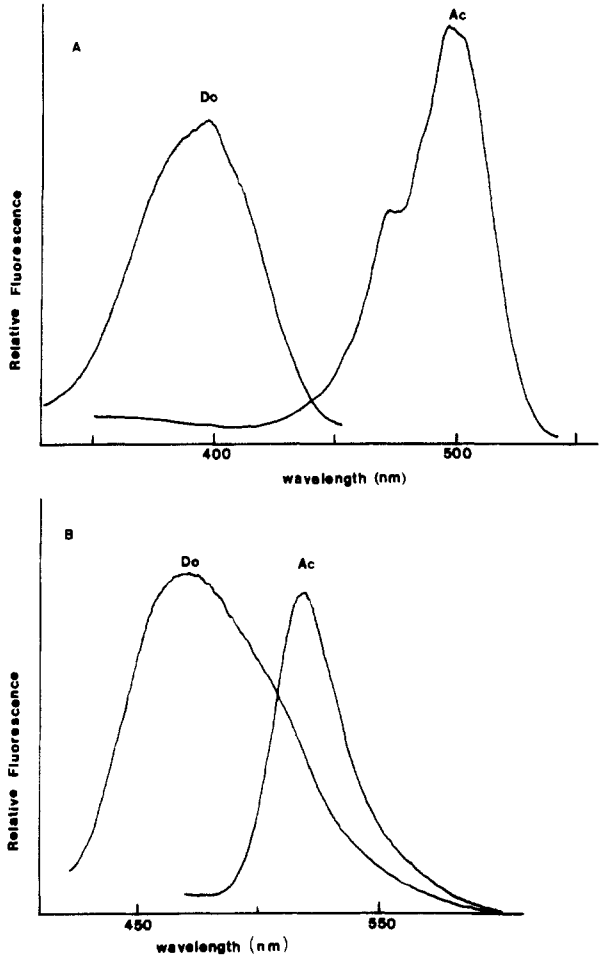

FIGURE 5: Uncorrected fluorescence spectra of MDPF- (Do) and fluorescein- (Ac) labeled E1 component. Excitation spectra are shown in (A) and emission spectra in (B). 40 μg/mL of the MDPF-labeled and 20 μg/mL of the fluorescein-labeled protein was used. Fluorescence sensitivity for MDPF is 3 times higher than for FITC.

Moe et al., 1974; Shepherd et al., 1976).

For the pyruvate dehydrogenase complex a diameter of 40 nm has been determined by small angle X-ray scattering, i.e., the circumference is about 125 nm (Durchschlag, 1975). Thus energy transfer between chromophores bound to different E1 molecules on the complex surface is confined to a maximum distance of $^1/_{20}$ of the circumference. On the assumption of an even distribution of the 16–24 E1 subunits on the complex molecule, fluorescence energy transfer should occur with significant efficiency only between nearest E1 neighbors. Using one donor-labeled E1 subunit as a marker bound to the E2E3 subcomplex, one is able to measure the binding of acceptor-labeled E1 subunits in the direct neighborhood by sensitized fluorescence. By this method it should be possible to determine the relative orientation of binding molecules to those already bound, thereby allowing conclusions about the progression of the reassembly.

We have used 2-methoxy-2,4-diphenyl-3(2*H*)-furanone (MDPF) as the donor chromophore and fluorescein isothiocyanate (FITC) as the acceptor chromophore. Both chromophores bind covalently to free amino groups of proteins. Under the conditions used in the labeling procedure, FITC should be preferentially attached to the N-terminal amino acid (Maeda et al., 1969). MDPF, which by itself is nonfluorescent, yields fluorescent pyrrolinones after reaction with free primary amino groups of the protein (Weigele et al., 1973).

Uncorrected fluorescence excitation and emission spectra of the enzyme-bound fluorophores are shown in Figure 5. The

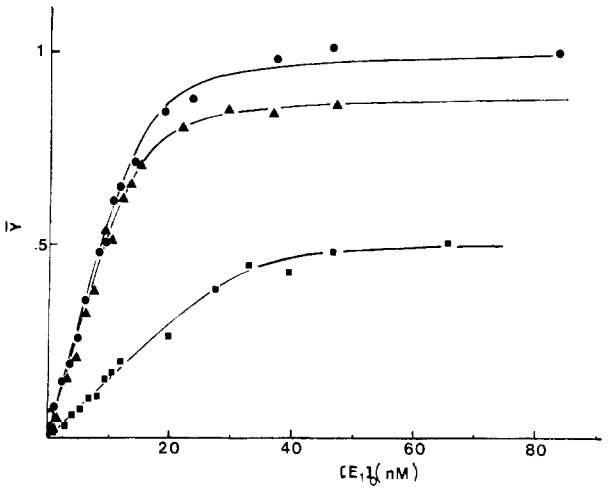

FIGURE 6: Saturation of the E2E3 subcomplex with dye-labeled E1 component. To 8.13 nM E2E3 subcomplex increasing amounts of E1 component were added, and the steady-state reaction rate of the reconstituted pyruvate dehydrogenase complex was plotted against the E1 monomer concentrations. (●) Native, (▲) fluorescein-labeled, and (■) MDPF-labeled E1 component.

MDPF conjugate exhibits a fluorescence emission maximum at 480 nm, whereas the fluorescein isothiocyanate labeled E1 shows an absorption band at 496 nm, so that partial spectral overlap occurs.

To follow energy transfer, we excited the donor-labeled protein at the absorption maximum of MDPF at 396 nm, and the increase in fluorescence intensity at 517 nm was measured upon the addition of acceptor-labeled subunit. Since the acceptor chromophore also absorbs at 396 nm, it was excited even in the absence of the donor; still an increase up to 15% in fluorescence intensity due to sensitized fluorescence was observed when the donor-labeled component was present. Whereas binding of the E1 subunits to the subcomplex is not impaired by the labeling with the chromophore, the enzyme component suffers a certain decrease in the activity as can be seen from Figure 6. This is more prominent after treatment of the enzyme with MDPF than with fluorescein isothiocyanate, since more MDPF must be coupled to E1 to yield a sufficiently high energy transfer signal.

To investigate the reassembly of the pyruvate dehydrogenase complex, we partially saturated the E2E3 subcomplex with donor-labeled subunits. Four different amounts of the donor-labeled enzyme component were chosen to yield saturation of the subcomplex in the range of 5–75%. Acceptor-labeled E1 was then added until complete saturation was achieved. As a control the whole procedure was repeated without addition of the subcomplex, so that no energy transfer should occur. The titration curves are shown in Figure 7. A linear increase in fluorescence intensity is observed in the control experiments due to the intrinsic fluorescence of the acceptor. In the presence of the subcomplex a much steeper increase of fluorescence intensity is seen. The binding function is obtained by subtraction of the control curve from the latter.

When the subcomplex was saturated up to 5%, i.e., one E1 polypeptide chain (on the average) is bound to one molecule of the E2E3 subcomplex, a clearly sigmoidal saturation function can be observed (Figure 7A). The same behavior is found when the amount of donor-labeled E1 was increased only slightly (Figure 7B).

However, when half-saturation of the subcomplex by the donor-labeled E1 component is already exceeded, the fluorescence energy transfer occurs immediately after addition of the acceptor-labeled subunit, and a hyperbolic rather than

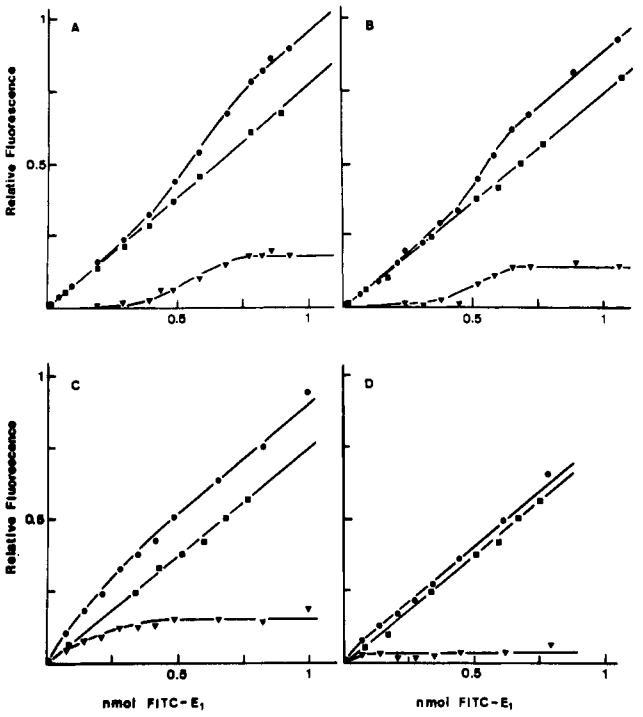

FIGURE 7: Fluorescence titration of E2E3 subcomplex with dye-labeled E1 component. MDPF-labeled E1 component was mixed with a constant amount of E2E3 subcomplex in 1 mL of 0.1 M potassium phosphate buffer, pH 7.6. Thereafter fluorescein-labeled E1 component was added stepwise at intervals of 5 min. Sensitized fluorescence emission was measured at 517 nm. Excitation was at 396 nm; temperature was maintained at 25 °C. The concentration of the components was low enough to avoid inner filter effects. Average degree of labeling of the components with the chromophores was 7.8 mol of MDPF/mol of E1 and 1.2 mol of fluorescein/mol of E1. The symbols in all diagrams are (●) titation curve, (■) control titration in absence of E2E3 subcomplex, and (▲) difference between both curves. Concentrations of MDPF-labeled E1 monomer and E2E3 protomer, respectively (the approximate degree of saturation is indicated in parenthesis), are as follows: (A) 8.5×10^{-8} M, 3.6×10^{-7} M (5%); (B) 3.9×10^{-7} M, 3.75×10^{-7} M (18%); (C) 5.9×10^{-7} M, 3.17×10^{-7} M (55%); (D) 8.9×10^{-7} M, 3.17×10^{-7} M (75%).

a sigmoidal saturation function is obtained (Figure 7C,D). From Figure 7A it is found that saturation is achieved when 1.8 polypeptide chains of the E1 component are bound to one E2E3 protomer.

Discussion

The question of whether the aggregation of proteins is necessary to attain catalytic activity is not yet solved for most of the known enzymes (Jaenicke et al., 1981). In the case of the pyruvate dehydrogenase complex from *E. coli* the situation seems clear insofar as the overall activity of the enzyme complex is strictly bound to the presence of all of its three different enzyme components. However, the isolated components still retain the ability to catalyze the partial reactions by which they contribute to the overall activity, and their catalytic properties are not greatly changed upon integration into the complex (Saumweber et al., 1981; Schmincke-Ott & Bisswanger, 1981).

In this study we tried to follow the reassembly of the pyruvate dehydrogenase complex from its subunits. Obviously the most simple way to do this is to follow the restoration of the overall enzymatic activity. This is not without problems, since the reactivation may be a complex process comprised of several reaction steps.

At first we were concerned to verify that the degree of regain of overall catalytic activity actually can serve as a direct measure for reassembly. Upon mixing of the components a considerable lag period is observed. Similar behavior has been reported for cytoplasmic pyruvate decarboxylase and transketolase from yeast (Hübner et al., 1978; Egan & Sable, 1981). Whereas these lags are interpreted as being due to thiamine diphosphate promoted oligomerization, including protein association and slow isomerization steps, it was demonstrated that for the case of the pyruvate dehydrogenase complex the rate of the reassociation process is independent of thiamine diphosphate (Bisswanger, 1974). Examination of the time constant τ_0 of this lag under conditions of pseudo-first-order kinetics demonstrates that a simple bimolecular reassembly mechanism can be excluded, since in this case a strict linear dependence of $1/\tau_0$ on the concentration of subcomplex is expected. The data fit, however, with a mechanism assuming a rapid binding of the E1 subunits to the subcomplex, followed by a slow isomerization step to yield the active enzyme.

The region of constant substrate utilization following the initial lag period in the progress curve indicates that, after the reassembly, a stable active enzyme complex is formed. This steady-state rate may therefore be taken as a direct measure for active enzyme complex.

An anticooperative binding of the E1 component to the E2E3 subcomplex was observed by steady-state measurements with an association constant of $K_{af} = 8 \times 10^7$ M^{-1} in the high saturation range. Due to the nonlinearity of the curve in the Stockell diagram, the association constant for the initial binding step cannot be obtained in this experiment. However, from the analysis of the lag period we obtained the constants for the formation of the complex $K_a^+ = k_1/k_{-1} = 1.5 \times 10^6$ M^{-1} as well as for the isomerization process $K_{ai} = k_2/k_{-2} = 2.4 \times 10^2$ M^{-1}, so that the overall association constant of the initial binding can be calculated to be $K_{a1} = k_1k_2/(k_{-1}k_{-2}) = 3.6 \times 10^8$ M^{-1}. Obviously a nearly 5-fold decrease in affinity for the E1 subunit to the subcomplex occurs during the saturation process. Cooperativity disappeared completely when the components were allowed to react with one another for a longer time before the steady-state rate was measured. This preincubation not only changes the binding function but also increases the association constant by a factor of more than 250. It may be assumed that initially an active but less stable complex is formed. This complex reshuffles to a more stable conformation with a half-life of 27 h (Hale et al., 1979) in a relatively slow process.

The anticooperative binding behavior as well as the change to normal binding after preincubation may account for the difficulties in determining the exact polypeptide chain stoichiometry of the pyruvate dehydrogenase complex from *E. coli*. While a ratio of 2:2:1 for the three different enzyme components E1:E2:E3 has been reported by Eley et al. (1972) and Angelides et al. (1979), Vogel et al. (1972a,b) and Bates et al. (1975) found a stoichiometry of >1:1:1. The latter authors reported a limiting chain ratio of 2:1:1. Binding of the E1 component occurs exclusively to the E2 subunits (Reed, 1974). The subcomplex was therefore assumed to consist of binding equivalents, protomers, containing one E2 and one E3 chain. Determination of the flavin content of the pyruvate dehydrogenase complex (Vogel et al., 1972b; H. Bisswanger, unpublished results) as well as aminidation of the polypeptide chains (Bates et al., 1975) suggests such a 1:1 ratio. Based on such a protomer with a molecular weight of 139 000, we found, at saturating conditions of the E1 component, that one E1 dimer binds to one E2E3 protomer, thus confirming a limiting stoichiometry of 2:1:1. Our data, however, are not compatible with the 2:2:1 ratio proposed by Eley et al. (1972), since a limiting stoichiometry of 3.2:2:1 would be obtained

taking a 1:0.5 protomer (M_r = 111 000).

In *E. coli*, however, neither a great surplus of free E1 subunits nor sufficient time for the slow isomerization exists. Therefore, the anticooperative binding is apparently relevant for the assembly in vivo. Variable numbers of E1 polypeptide chains found in the native complex may thus in fact be caused by the formation of varying amounts of this component under different growth conditions (Henning et al., 1972). The heterogeneity previously found for the molecular weight of the native enzyme complex (Gilbert & Gilbert, 1980; Schmitt & Cohen, 1980) is in accordance with this assumption.

The anticooperativity observed in the kinetic experiments may be due to changes of the catalytic rate constant in the course of the reassembly process or to slow transitions of the catalytic active enzyme conformation (Frieden, 1970; Schramm & Morrison, 1971; Neet & Ainslie, 1980). However, we were able to demonstrate the anticooperative binding behavior of the E1 subunit to the E2E3 subcomplex directly by measurements of fluorescence energy transfer between neighboring E1 subunits.

Since by the technique employed only binding of subunits next to a prebound subunit is regarded, the resultant binding functions differ essentially in shape from those obtained by other methods. Three types of binding may be expected, i.e., normal, cooperative, or anticooperative. In the cooperative mode, binding adjacent to another E1 subunit should be preferred, and energy transfer should be very efficient in the low saturation range. On the other hand energy transfer in the anticooperative case is restricted to higher levels of saturation because of favorable binding to sites without a neighboring E1 subunit at low saturation. Binding curves of these types were simulated by the Monte-Carlo method. A value of 20 identical binding sites arranged on a disk-shaped molecule was chosen. The disk shape is a rather crude simplification of the spacial structure of the E2E3 subcomplex as is the assumption of 20 binding sites. Since our experiments allow no conclusion about the absolute number of E2 chains actually present in the subcomplex, we took the mean between 16, as was proposed by Vogel et al. (1972b), and 24, stated by Reed et al. (1975), Angelides et al. (1979), Danson et al. (1979), and Fuller et al. (1979). However, neither the simplification of the complex structure nor the exact number of binding sites is very relevant for binding analysis by this method. Here we only aim to describe the general features of saturation curves since an exact fitting would require more detailed parameters than are known so far. In this procedure we assume that the occupation of isolated, independent binding sites always occurs with equal probability, while the occupation of sites adjacent to bound E1 occurs with a different probability, reflecting the assumption of cooperative or anticooperative binding (Figure 8). In counting the E1 pairs, only one possible pair was accepted, since we also assume that one subunit would take part in the energy transfer from one neighbor only. This also is not an essential point in the model, since even by including the possibility of forming pairs in two directions we would obtain basically the same kind of binding curves.

With this simulation, sigmoidal curves are obtained for anticooperative binding of the subunits, as actually observed in the experiments. If the binding of the E1 subunits proceeds in such an anticooperative manner, preincubation of the E2E3 subcomplex with a higher number of donor-labeled E1 subunits should result in an occupation of the isolated sites, leaving only sites adjacent to bound E1 available for further saturation. Now all acceptor-labeled subunits additionally bound should

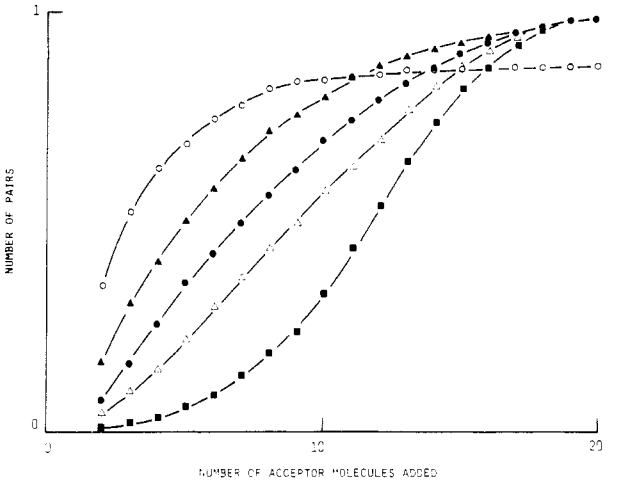

FIGURE 8: Monte-Carlo simulation of the binding of the pyruvate dehydrogenase component to the E2E3 subcomplex, assuming different mechanisms. One molecule of the free component (donor) was added to one molecule of subcomplex. Acceptor-labeled component was added stepwise up to saturation, and the subunit pairs formed with the donor were counted after each step. The relative probability of occupation of isolated (unhindered) binding sites was taken to be unity in all cases, while that for occupation of neighboring (hindered) sites was assumed to be 1 (●, normal binding), 2 (▲), 20 (○, cooperative binding), 0.5 (△), or 0.1 (■, anticooperative binding).

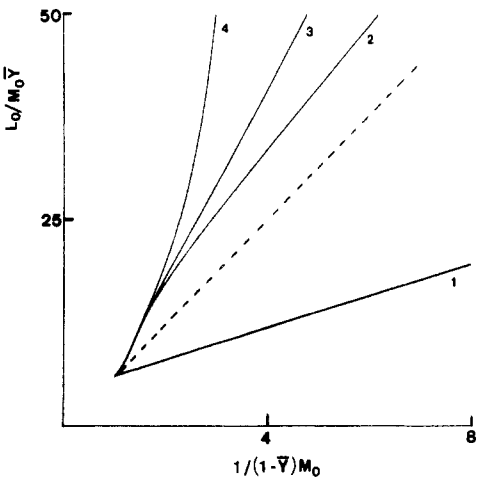

FIGURE 9: Simulation of anticooperative binding behavior in the Stockell diagram. The curves were computed for a protein consisting of four identical subunits; the concentration of the subunits of the macromolecule is chosen to be $M_0 = 1$. The fractional saturation $\bar{Y}$ was calculated from eq 12 for increasing ligand concentrations (L). L_0 was calculated from $L_0 = L + 4\bar{Y}$. Origin and slopes of the curves were checked according to eq 13–16. (Curve 1) Normal binding, the association constants for the four individual binding steps are $K_1 = 2$, $K_2 = 3/4$, $K_3 = 1/3$, and $K_4 = 1/8$. (Curves 2–4) Anticooperative binding ($K_1 = 2$; $K_2 = 0.2$; $K_3 = 0.0889$); K_4 is varied as 0.0333 (curve 2), 0.02 (curve 3), and 0 (curve 4). The dotted line indicates the limiting slope for $\bar{Y} \rightarrow 0$ and is obtained from eq 15.

contribute to the energy transfer signal, thus giving rise to a hyperbolic binding function. Such curves are indeed found under these conditions.

There are several ways to account for the anticooperative binding mechanism. Applying the model for allosteric enzymes of Koshland et al. (1966), we obtained binding functions of this type, assuming negative cooperativity. However, in this model the change to normal binding behavior cannot be explained satisfactory. Inherently different binding sites, giving rise to similar binding curves, may be excluded for the same reason. Anticooperative binding may be elicited by direct steric hindrance of subunit binding. McGhee & von Hippel (1974) and Schwarz (1977) point out that the binding of a large

ligand to a macromolecule can cause partial occlusion of potential binding sites, thus giving rise to nonlinear secondary binding plots. The actual degree of binding will depend not only on the number of ligands bound but also on the distribution of these ligands. Indeed the E1 subunit is an extremely large ligand, and some steric disturbance of the binding of E1 subsequently is not unlikely (Reed et al., 1975). Elimination of this steric disturbance by time-dependent rearrangement leads to the appearance of normal binding behavior.

Acknowledgments

We thank Professor D. Mecke and Dr. W. Wright for valuable discussions and G. Knödler for help in the preparation of the manuscript.

Appendix

Cooperative effects in ligand binding are frequently analyzed by employing Hill or Scatchard plots. However, when concentration of unbound ligand cannot directly be determined as is the case for spectroscopic titrations, these plots are not so useful.

In these cases binding behavior may be characterized by plotting $1/[M_0(1-\bar{Y})]$ vs. $L_0/(M_0\bar{Y})$ as proposed by Stockell (1959), where M_0 is the initial concentration of the macromolecule, L_0 is the initial concentration of the ligand, and $\bar{Y}$ is the number of moles of ligand bound per mole of binding site.

For normal, noncooperative binding a linear relationship is obtained:

$$\frac{L_0}{M_0}\frac{1}{\bar{Y}} = n + \frac{1}{K_a}\frac{1}{M_0(1-\bar{Y})} \tag{11}$$

where n is the number of binding sites and K_a is the intrinsic association constant.

For a general treatment of binding behavior in the Stockell plot $\bar{Y}$ is defined from the equation of Adair (1925):

$$\bar{Y} = \frac{L_{bound}}{nM_0} = \frac{1}{n}\frac{\sum_1^n i\gamma_i L^i}{1+\sum_1^n \gamma_i L^i} \tag{12}$$

where L is the concentration of the free ligand and $\gamma_i = \prod_{j=1}^{j=i} K_j$ are the Adair constants. Computer simulations of some anticooperative binding curves are shown in Figure 9.

Origin of the Curves. For $\bar{Y} \to 0$ the limiting value of the abscissa will be $1/M_0$. The corresponding ordinate value ω is

$$\omega = \lim_{\bar{Y}\to 0}\frac{L_0}{M_0\bar{Y}} = \lim_{L\to 0} n + \frac{n}{M_0}\frac{1+\sum_1^n \gamma_i L^i}{\sum_1^n i\gamma_i L^{i-1}} = n + \frac{n}{M_0\gamma_1} \tag{13}$$

By employing stoichiometric association constants (K_i) or statistically corrected (intrinsic) association constants (K_i'), we obtain

$$\omega = n + \frac{n}{M_0K_1} = n + \frac{1}{M_0K_1'}$$

Thus the origin of the curves in the Stockell plot has the coordinates $1/M_0$ and $n + 1/(M_0K_1')$.

Slope of Binding Curves in the Stockell Plot. The slope (sl) in the Stockell plot is

$$\mathrm{sl} = \frac{\mathrm{d}[L_0/(M_0\bar{Y})]}{\mathrm{d}(1/[M_0(1-\bar{Y})])}$$

By employing the Adair equation (12) and the substitution $L_0 = L + nM_0\bar{Y}$, this can be solved analytically. The following expression is obtained:

$$\mathrm{sl} = \{n[(\sum_1^n i\gamma_i L^{i-1})^2 - (1+\sum_1^n \gamma_i L^i)\sum_1^n i(i-1)\gamma_i L^{i-2}][n + n\sum_1^n \gamma_i L^i - \sum_1^n i\gamma_i L^i]^2\}/\{[\sum_1^n i\gamma_i L^{i-1}]^2[n\sum_1^n i\gamma_i L^{i-1}(n + n\sum_1^n \gamma_i L^i - \sum_1^n i\gamma_i L^i)] - [n(1+\sum_1^n \gamma_i L^i)(n\sum_1^n i\gamma_i L^{i-1} - \sum_1^n i^2\gamma_i L^{i-1})]\} \tag{14}$$

From this the slopes at very high degrees of saturation (sl_∞) and very low degrees of saturation (sl_0) can be calculated:

$$\mathrm{sl}_0 = \lim_{L\to 0}\text{slope} = n^2\frac{\gamma_1^2 - 2\gamma_2}{\gamma_1^3} = n^2\frac{K_1 - 2K_2}{K_1^2} = \frac{nK_1' - (n-1)K_2'}{(K_1')^2} \tag{15}$$

$$\mathrm{sl}_\infty = \lim_{L\to\infty}\text{slope} = \frac{1}{n}\frac{\gamma_{n-1}}{\gamma_n} = \frac{1}{nK_n} = \frac{1}{K_n'} \tag{16}$$

In case of normal binding ($K_1' = K_2' = K_n' = K$), $\mathrm{sl}_0 = \mathrm{sl}_\infty = 1/K$. For anticooperative binding $K_{i+1}' < K_i'$. From eq 15 and 16 it is easily demonstrated that

$$\mathrm{sl}_0 > 1/K_1' \geq 1/K \qquad \mathrm{sl}_\infty > 1/K_1' \geq 1/K$$

i.e., the limiting slopes for anticooperative binding are positive and steeper than the slope in the noncooperative case, as is seen in Figure 9.

References

Adair, G. S. (1925) *J. Biol. Chem. 63*, 529–545.
Angelides, K. J., Akiyama, S. K., & Hammes, G. G. (1979) *Proc. Natl. Acad. Sci. U.S.A. 76*, 3279–3283.
Bates, D. L., Harrison, R. A., & Perham, R. N. (1975) *FEBS Lett. 60*, 427–430.
Bates, D. L., Danson, M. J., Hale, G., Hooper, E. A., & Perham, R. N. (1977) *Nature (London) 268*, 313–316.
Bisswanger, H. (1974) *Eur. J. Biochem. 48*, 377–387.
Bisswanger, H. (1981) *J. Biol. Chem. 256*, 815–822.
Danson, M. J., Hale, G., Johnson, P., Perham, R. N., Smith, J., & Spragg, P. (1979) *J. Mol. Biol. 129*, 603–617.
Durchschlag, H. (1975) *Biophys. Struct. Mech. 1*, 169–188.
Egan, R. M., & Sable, H. Z. (1981) *J. Biol. Chem. 256*, 4877–4883.
Eley, M. H., Namihara, G., Hamilton, K., Munk, P., & Reed, L. J. (1972) *Arch. Biochem. Biophys. 152*, 655–669.
Fernandez-Moran, H., Reed, L. J., Koike, M., & Willms, C. R. (1964) *Science (Washington, D.C.) 145*, 930–932.
Förster, T. (1948) *Ann. Phys. (Leipzig) 2*, 55–75.
Frieden, C. (1970) *J. Biol. Chem. 245*, 5788–5799.
Fuller, C. C., Reed, L. J., Oliver, R. M., & Hackert, M. L. (1979) *Biochem. Biophys. Res. Commun. 90*, 431–438.
Gilbert, G. A., & Gilbert L. M. (1980) *J. Mol. Biol. 144*, 405–407.
Gutfreund, H. (1972) *Enzymes: Physical Principles*, pp 222–228, Wiley, New York.
Hale, G., Bates, D. L., & Perham, R. N. (1979) *FEBS Lett. 104*, 343–346.
Hammersley, J. M., & Handscomb, D. C. (1965) *Monte Carlo Methods*, Methuen, London.
Handschin, U. E., & Ritschard, W. J. (1976) *Anal. Biochem. 71*, 143–155.
Hartree, E. F. (1972) *Anal. Biochem. 48*, 422–427.
Henning, U., & Herz, C. (1964) *Z. Vererbungsl. 95*, 260–275.

Henning, U., Vogel, O., Busch, W., & Flatgaard, J. E. (1972) *Protein-Protein Interactions* (Helmreich, E., & Jaenicke, R., Eds.) pp 343–364, Springer, Berlin.
Hübner, G., Weidhase, R., & Schellenberger, A. (1978) *Eur. J. Biochem. 92*, 175–181.
Jaenicke, R., Vogel, W., & Rudolph, R. (1981) *Eur. J. Biochem. 114*, 525–531.
Klotz, I. M. (1946) *Arch. Biochem. 9*, 109.
Koike, M., Reed, L. J., & Carroll, W. R. (1963) *J. Biol. Chem. 238*, 30–39.
Koshland, D. E., Jr., Némethy, G., & Filmer, D. (1966) *Biochemistry 5*, 365–385.
Lowry, O. H., Rosebrough, N. J., Farr, A. L., & Randall, R. J. (1951) *J. Biol. Chem. 193*, 265–375.
Maeda, H., Ishida, N., Kawauchi, H., & Tuzimura, K. (1969) *J. Biochem. (Tokyo) 65*, 777–783.
McGhee, J. D., & von Hippel, P. H. (1974) *J. Mol. Biol. 86*, 469–489.
Moe, O. A., Lerner, D. A., & Hammes, G. G. (1974) *Biochemistry 13*, 2552–2557.
Neet, K. E., & Ainslie, G. R. (1980) *Methods Enzymol. 64*, 192–226.
Perham, R. N., & Thomas, J. O. (1971) *FEBS Lett. 15*, 8–12.
Perham, R. N., & Hooper, E. A. (1977) *FEBS Lett. 73*, 137–140.
Reed, L. J. (1974) *Acc. Chem. Res. 7*, 40–46.
Reed, L. J., Pettit, F. H., Eley, M. H., Hamilton, L., Collins, J. M., & Oliver, R. M. (1975) *Proc. Natl. Acad. Sci. U.S.A. 72*, 3068–3072.
Rinderknecht, H. (1962) *Nature (London) 193*, 167–168.
Saumweber, H., Binder, R., & Bisswanger, H. (1981) *Eur. J. Biochem. 114*, 407–411.
Schmincke-Ott, E., & Bisswanger, H. (1981) *Eur. J. Biochem. 114*, 413–420.
Schmitt, B., & Cohen, R. (1980) *Biochem. Biophys. Res. Commun. 93*, 709–712.
Schramm, V., & Morrison, J. F. (1971) *Biochemistry 10*, 2272–2277.
Schwartz, E. R., Old, L. O., & Reed, L. J. (1968) *Biochem. Biophys. Res. Commun. 31*, 495–500.
Schwarz, G. (1977) *Biophys. Chem. 6*, 65–76.
Scouten, W. H., Lubcher, R., & Baughman, W. (1974) *Biochim. Biophys. Acta 336*, 421–426.
Shepherd, G. B., Papadakis, N., & Hammes, G. G. (1976) *Biochemistry 15*, 2888–2893.
Stockell, A. (1959) *J. Biol. Chem. 234*, 1286–1292.
Strickland, S., Palmer, G., & Massey, V. (1975) *J. Biol. Chem. 250*, 4048–4052.
Stryer, L., & Haugland, R. P. (1967) *Proc. Natl. Acad. Sci. U.S.A. 58*, 719–726.
Tengerdy, R. P., & Chang, C. (1966) *Anal. Biochem. 16*, 377–388.
Vogel, O. (1977) *Biochem. Biophys. Res. Commun. 74*, 1235–1241.
Vogel, O., & Henning, U. (1971) *Eur. J. Biochem. 18*, 103–115.
Vogel, O., Hoehn, B., & Henning, U. (1972a) *Eur. J. Biochem. 30*, 354–360.
Vogel, O., Hoehn, B., & Henning, U. (1972b) *Proc. Natl. Acad. Sci. U.S.A. 69*, 1615–1619.
Weigele, M., De Bernardo, S., Leimgruber, W., Cleeland, R., & Grunberg, E. (1973) *Biochem. Biophys. Res. Commun. 54*, 899–906.

Molecular Topography of Phytochrome As Deduced from the Tritium-Exchange Method†

Tae-Ryong Hahn and Pill-Soon Song*

ABSTRACT: The hydrogen–tritium-exchange measurements on phytochrome have been performed to detect the conformational differences between the red-absorbing (Pr) and the far-red-absorbing (Pfr) forms of phytochrome. The large and small Pfr molecules revealed more exchangeable protons than did the corresponding Pr molecules by 96 and 70 protons, respectively. These results suggest that the Pr → Pfr phototransformation is accompanied by an additional exposure of the peptide chains in the Pfr molecule. Of 1682 theoretically exchangeable hydrogens in undegraded phytochrome, only 442 (26%) and 346 (21%) protons were found to be exchangeable (excluding instantaneously exchangeable protons that cannot be determined by the present method). Thus, the phytochrome protein appears to be compact and highly folded. The kinetic analyses of the tritium exchange-out curves indicate that two kinetically different groups are responsible for the conformational differences between the Pr and Pfr forms of phytochrome. These components are due to (1) the exposure of hydrogen-bonded peptide segments (α helix and/or β-pleated sheet) in the chromophore vicinity of Pfr and (2) the exposure of hydrogen-bonded peptide segments on the chromophore peptide domain as well as on the chromophore-free tryptic domain of undegraded phytochrome.

Phytochrome mediates a variety of the morphogenic and developmental responses of higher plants to red light. There are two forms of phytochrome, an inactive red-absorbing form (Pr)[1] and an active far-red-absorbing form (Pfr). The latter is formed from the former by red light [see reviews by Kendrick & Spruit (1977), Pratt (1978), and Rüdiger (1980)].

From detailed spectroscopic analyses of the absorption spectra of Pr and Pfr, it was concluded that the chromophores of both phytochrome forms possess largely similar conformations, excluding a *gross* isomerization of the chromophore

† From the Department of Chemistry, Texas Tech University, Lubbock, Texas 79409. *Received October 13, 1981.* This work was supported in part by the Robert A. Welch Foundation (D-182) and the National Science Foundation (PCM79-06806).

[1] Abbreviations: EDTA, ethylenediaminetetraacetic acid; Pfr, far-red-absorbing form of phytochrome; Pr, red-absorbing form of phytochrome; $NaDodSO_4$, sodium dodecyl sulfate; ANS, 8-anilinonaphthalene-1-sulfonate.

0006-2960/82/0421-1394$01.25/0